THE JOURNAL OF PHYSICAL CHEMISTRY A LETTERS

2009, *113,* 3427–3430
Published on Web 03/24/2009

Nonadiabatic Mixed Quantum−Classical Dynamic Simulation of π-Stacked Oligophenylenevinylenes

Fabio Sterpone

Department of Chemistry, École Normale Supérieure, 24 rue Lhomond, F75231 Paris CEDEX 05, France

Michael J. Bedard-Hearn

Department of Chemistry and Biochemistry, University of Texas, Austin, Texas 78712

Peter J. Rossky*

Department of Chemistry and Biochemistry and Institute for Computational Engineering and Sciences, University of Texas, Austin, Texas 78712

Received: February 10, 2009

We present results from the first nonadiabatic (NA), nonequilibrium mixed quantum−classical molecular dynamics simulations of π-stacked oligophenylvinylene (OPV) chains with a quantum electronic Hamiltonian (Pariser−Parr−Pople with excited states given by configuration interaction) that goes beyond the tight-binding approximation. The chains pack ∼3.6 Å apart in the ground state at 300 K, and we discuss how thermal motions, chiefly a relative sliding motion along the oligomer backbone, affect the electronic structure. We assign the electronic absorption spectrum primarily to the $S_0 \rightarrow S_2$ transition as transitions from the ground state to S_1 and S_3 are particularly weak. After photoexcitation, the system rapidly decays via NA transitions to S_1 in under 150 fs. On S_1, the system relaxes as a bound exciton, localized on one chain that may hop between chains with a characteristic time between 300 and 800 fs. We find that the system does not make a rapid transition to the ground state because both the NA and radiative couplings between S_1 and S_0 are weak.

The molecular arrangement of conjugated polymers (CPs) plays a central role in determining the optoelectronic properties of devices made from thin films. Understanding the interchain interactions of polymers in films is a key step toward increased efficiency of devices and design of optimal thin films.[1,2] Here, we characterize the electronic ground- and excited-state properties of two π-stacked polyphenylvinylene (PPV) oligomers in terms of their structure and dynamics.

For two π-stacked cofacial stilbene molecules (PPV with just two repeat units), Cornil et al.[3] showed that the ground-to-first-excited-state transition, $S_0 \rightarrow S_1$, is dipole-forbidden. In an ideal geometry, the transition to S_1 is said to be symmetry-"forbidden", a result that persists for longer oligomers. There is also an energy-level splitting between S_1 and S_2 whose magnitude is affected by the relative spacing between chains; the nature of the forbidden transition to S_1, however, remains unchanged as a function of separation.[2,4−6] It has been inferred that such a symmetry-forbidden transition is the origin of luminescence quenching observed experimentally in aggregated polymers[4,7] compared to single chains.

The effects of interchain interactions have also been studied in other CP systems,[7] as well as PPV oligomers of different sizes[5] and interchain configurations. In short, conformational changes that remove the inversion symmetry of the ideal cofacial arrangement allow S_1 to borrow intensity from other states. Calculations of both sexithienyl (6T) arranged in a herringbone fashion[7] and π-stacked PPV with a relative planar rotation[4] showed enhanced coupling to S_1 from the ground state, providing a possible mechanism to reduce luminescence quenching.

Despite this progress, key questions remain about the optoelectronic properties of aggregated CP systems. Chain arrangement in films, for example, is almost certainly neither a herringbone nor a simple cofacial configuration. Additionally, it is not yet known how thermal fluctuations of the chains contribute to symmetry breaking or how the dynamics and structure of photoexcited CPs differ from the those in the ground state.

In this Letter, we present the results of equilibrium (adiabatic) and nonequilibrium (nonadiabatic) mixed quantum−classical (MQC) molecular dynamics (MD) simulations of a pair of π-stacked oligophenylenevinylene (OPV) pentamers, denoted as 2×(5)OPV.[8−10] We show that the shape of the ground-state (GS) absorption spectrum is determined primarily by thermal dynamics of the polymer backbone, notably, a relative translation that switches the π-stacking interactions between phenyl−phenyl and phenyl−vinyl overlap. The calculated absorption spectrum concentrates oscillator strength in the transition to the second excited state, S_2,[4,7] but we also find weak transitions to S_1 and S_3, the result of thermal symmetry breaking. We use nonadiabatic (NA) MD trajectories to explore the relationship between photoluminescence and the dynamics of the polymers following

* To whom correspondence should be addressed.

10.1021/jp901229z CCC: $40.75

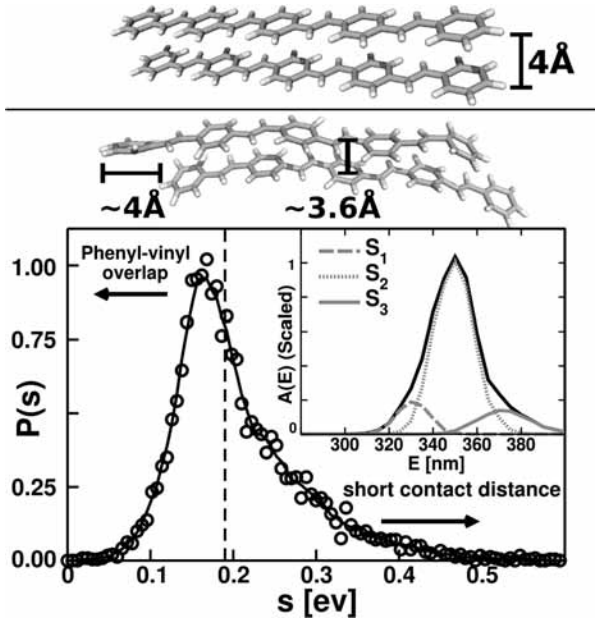

Figure 1. Top Panels: Rendering of the π-stacked (5)OPV dimer in the initial configuration and with enhanced phenyl−vinyl overlap showing a lateral displacement of ~ 4 Å.[31] Lower Panel: Relative probability distribution, $P(s)$, of the electronic energy-level splitting, s, between the two lowest excited states, $s = E_{20} - E_{10}$. The vertical dashed line indicates the value of s for the initial configuration; the curve running through the data is a five-point box-car average to guide the eye. Inset: Simulated thermal (300 K) absorption spectrum of 2×(5)OPV (black curve), composed of transitions from the ground state to the first three excited states, S_1, S_2, and S_3 (gray curves). Line shapes are the envelopes of the distribution of instantaneous transitions from the ground-state simulation.

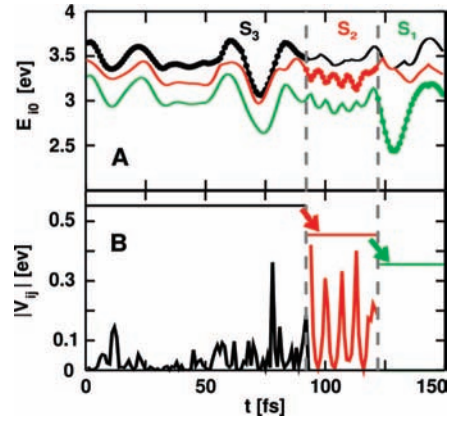

Figure 2. Example nonadiabatic trajectory for 2×(5)OPV initialized in S_3. Panel A shows the adiabatic energy gap, E_{i0}, as a function of time after excitation (solid curves, filled circles, and labels indicate currently occupied state); nonadiabatic transitions between the states occur at times marked by vertical dashed lines. Panel B shows the magnitude of the nonadiabatic coupling matrix element, $|V_{ij}|$ (eq 1), between states i (the currently occupied state) and $j = i - 1$ (e.g., the black curve is $|V_{32}|$) for the same trajectory as that in Panel A. On this scale, V_{10} is not discernible.

photoexcitation. We find that the system undergoes an ultrafast (sub-150 fs) relaxation to S_1, where it re-equilibrates to a significantly different geometry, relative to 2×(5)OPV in the GS. This lattice distortion in aggregated PPV systems contributes to the lengthy excited-state lifetimes observed experimentally,[11,12] as confirmed by our 9 ps NA runs, which do not return to the ground state because of poor NA coupling.

We use a MQC MD scheme that combines the quantum (π-electron) degrees of freedom in the form of the semiempirical Pariser−Parr−Pople Hamiltonian[13−15] with a fully flexible mechanical model[10,16] for the classical (nuclear) degrees of freedom. The adiabatic excited states are given by the single-excitation configuration interaction (SCI) procedure[4,7,16,17] calculated in a finite active space of the first 50 states.[18] The influence of the π-electrons on the nuclei (i.e., the forces acting on the OPV backbone from the π-system) in the ground and excited states is described in detail elsewhere.[8,19] We integrate the classical dynamics with a 1 fs time step in a velocity Verlet routine.[20] The initial GS configuration is a cofacial (5)OPV dimer separated by 4 Å (top panel, Figure 1). Prior to collecting statistics, the system equilibrated at 300 K for 30 ps with velocity rescaling every 200 fs. After equilibration, we performed a single constant-energy 100 ps GS trajectory.

To study the excited-state dynamical relaxation of the system, we performed eight nonequilibrium NA trajectories, each of which simulated a one-photon vertical excitation. The π-system is instantaneously promoted from the ground state into the second or third excited state, with initial configurations (each separated by at least 10 ps) taken directly from the GS trajectory. The photoexcited system evolves adiabatically (on one electronic surface) with one or more stochastic switches (NA transitions) between electronic states governed by the surface-hopping method.[21,22]

We begin our discussion by examining the GS electronic absorption spectrum shown in the inset of Figure 1. The spectrum is calculated without contributions from an ad hoc line broadening.[3] Rather, its shape is entirely associated with thermal inhomogeneous broadening. The GS absorption spectrum (black curve) is shown as a superposition of transitions to only the first three excited states (gray curves)[23] and peaks at ~350 nm, corresponding to the $S_0 \rightarrow S_2$ transition. The $S_0 \rightarrow S_1$ transition is relatively weak, with an average oscillator strength that is seven times less than that to S_2, but it is not totally "forbidden." The shoulder at 330 nm is from the somewhat weak $S_0 \rightarrow S_3$ transition. A charge- transfer state has been observed ~0.1−0.3 eV above the optically active state in several CP systems, PPV dimers[24,25] and 6T[7] included; however, we cannot make that assignment of S_3 here. Such a state would involve a transition between the chains, and here, the $S_0 \rightarrow S_3$ transition dipole moment is polarized along the PPV backbones with no interchain components.[26] We conclude that the three lowest singlet excited states are bound excitons, as for the lowest excited states in isolated oligomers.[10]

It was shown previously that the first two excited states for short oligomers[3,4] change as a function of separation, d. For stilbene,[3] S_1 and S_2 are degenerate in energy for $d \geq 15$ Å, but the energy splitting $s = E_{20} - E_{10}$ (where E_{i0} represents the adiabatic energy gap between the ground and ith excited states) increases to 0.25 eV at $d = 4$ Å[4] (using the INDO Hamiltonian with SCI). We find that the dynamics of the two chains in the GS at 300 K results in an asymmetric distribution of s. Figure 1 shows the normalized probability distribution, $P(s)$, which is a histogram of the instantaneous values of s over the 100 ps GS trajectory; the dashed line at 0.19 eV is for the initial unequilibrated configuration (top panel). $P(s)$ peaks at 0.16 eV with a long tail to high s that is correlated with close packing of the chains and lower values of s that are generally correlated with configurations with enhanced phenyl−vinyl interactions between the chains (middle panel, Figure 1); both mirror changes in molecular orbital overlap. The contact distance fluctuates around 3.6 ± 0.1 Å on a ~1 ps time scale, and the thermal

axial sliding dynamics (that alters the phenyl−vinyl overlap) shows a maximal displacement of about 4 Å with a period of ∼10−15 ps.[27]

To study the role of structure and dynamics in the excited states of 2×(5)OPV, we turn to the series of NA nonequilibrium simulations, initiated to the second or third excited state (four independent configurations for each state). Following excitation, the system undergoes rapid NA relaxation to S_1, making the transition from S_2 in ∼40−100 fs. There are no transitions back to S_2, and the system quickly reaches a steady fluctuating energy on S_1 after about 50 fs. A similar process occurs when initiating to S_3; we observe rapid sequential decay to S_1 through S_2 (see Figure 2A). Figure 2A shows the adiabatic energy gaps, E_{i0}, as a function of time following excitation. In each of the four S_3 trajectories, S_2 was reached in under 100 fs, and the transition to S_1 occurred almost immediately (between 10 and 30 fs later).

The coupling to S_0 from S_1 is found to be orders of magnitude smaller than that from S_2 to S_1; hence, the system does not relax to S_0 even after 9 ps. This is demonstrated in Figure 2B, which shows the magnitude of the electronic NA coupling matrix elements

$$V_{ij} = -i\hbar(\vec{d}_{ij}\cdot\dot{\vec{R}}) \quad (1)$$

for the same trajectory as that shown in Figure 2A. V_{ij} transfers amplitude from adiabatic state i to j via the dynamics of the classical nuclei, $\vec{R}$, where $\vec{d}_{ij}$ is the nonadiabatic coupling vector.[19] In general, we find NA transitions occur when the coupling strength, $|V_{ij}|$, spikes; here, $|V_{32}| \sim 0.2$ eV just before the transition at ∼90 fs. The system undergoes a transition to S_1 about 30 fs later with a similar coupling magnitude;[28] $|V_{01}|$ is not discernible on this scale, and we do not observe NA relaxation to S_0.

In addition to the poor nonradiative relaxation rate, recall that the radiative transition $S_1 \rightarrow S_0$ is symmetry-forbidden in idealized structures. We find that upon re-equilibration on S_1, the transition dipole moment for the $S_1 \rightarrow S_0$ transition increases by a factor of 2, although radiative coupling remains reduced by ∼50% when compared to that of an isolated (5)OPV oligomer.[10] Combined, these two results are consistent with extended excited-state lifetimes and poor fluorescence yields in aggregates.[11,12]

We now turn to the underlying nuclear structure of the 2×(5)OPV system. In our previous paper, we showed that a ring order parameter, d_R (eq 15 in ref 10), can be used to track the effect of the exciton on the oligomer's nuclear coordinates (lattice). The order parameter compares the π-bonds in each constituent ring, giving $d_R = 0$ for a perfect hexagon and a positive fraction for quinoid-like structures. We found for (10)OPV that d_R was, on average, ∼0.19 Å in the ground state and ∼0.40 Å in the excited state. Although thermal fluctuations allow the S_1 exciton to sample (and thus distort) all rings, it generally localizes in the middle of the chain and is spread across three or four repeat units; the terminal rings, on average, distort the least.

Figure 3 shows a time trace of $(d_R)^2$ for 2×(5)OPV as a contour plot from a trajectory run on the first excited state, S_1. As is the case for an isolated oligomer, the exciton induces a quinoidal distortion on a few rings near the middle of a single chain; this perturbation to the lattice prevents the system from making a NA transition back to the ground state. In addition, we find that the close packing of the two chains allows the exciton to hop between the chains, with a residency time of

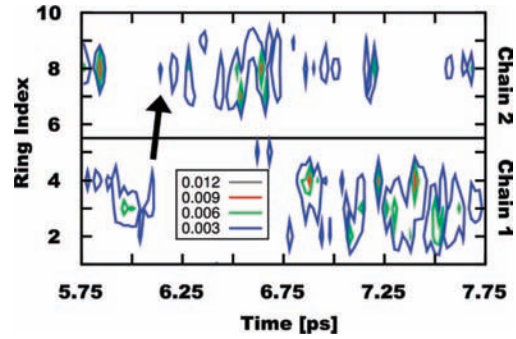

Figure 3. Contour plot of the ring order parameter squared, d_R^2 (eq 15 in ref 10) for a single trajectory run on the S_1 surface as a function of time after simulated photoexcitation. The contours show how the rings in a (5)OPV dimer deviate from an idealized benzoid hexagon ($d_R^2 = 0$), with larger values indicating a quinoid-like distortion; we use it here as an indicator of singlet exciton localization. The arrow at $t \sim 6.25$ ps indicates the exciton hopping from chain 1 to 2; the units are Å^2.

∼500 fs. An example of such a hop from chain 1 to chain 2 is indicated by the arrow at $t \sim 6.25$ ps. Exciton hopping is not unexpected as the thermal motions of the polymers can always break symmetry, making one chain more hospitable to the exciton than the other. Previous quantum chemical calculations[4] on 2×(5)OPV for an energy-minimized S_1 geometry revealed an excitation that affects a single chain only for separations of $d \geq 10$ Å, whereas for separations less than 4 Å, the exciton was delocalized over the both chains, though not evenly.

In this study, we investigated the ground- and excited-state dynamical behavior of a π-stacked (5)OPV dimer. We showed how thermal motions perturb the symmetric cofacial configuration and that fluctuations of the contact distance, the between-chain overlap, and internal geometry induce an asymmetric distribution of the electronic energy splitting between S_1 and S_2. These dynamics also allow the transitions from the GS to S_1 and S_3 to gain oscillator strength. Thus, the absorption spectrum is assigned to a superposition of a strong transition to S_2 at 350 nm, plus a pair of weak transitions to S_1 and S_3. We found that the oscillator strength for $S_0 \rightarrow S_1$ is ∼7 times smaller than that between $S_0 \rightarrow S_2$, consistent with other calculations of CPs[3,4] and experimental studies.[29] The substantial nonadiabatic coupling between S_3 and S_2 and between S_2 and S_1 seen here is also consistent with time-resolved experiments showing ultrafast intramolecular relaxation.[30]

Once in the first excited state, we observed weak radiative coupling that is consistent with the long fluorescence lifetimes (∼1 ns) observed experimentally[11,12] and consistent with H-aggregate character.[12] Such weak coupling originates from the fact that the $S_1 \rightarrow S_0$ transition is symmetry-forbidden in idealized structures.[4] Re-equilibration on S_1 increases the transition dipole moment for the $S_1 \rightarrow S_0$ transition, but it is still relatively weak. Consistent with earlier inferences,[3,4,12] this reduced possibility of radiative relaxation is likely the quenching mechanism in polyphenylenevinylene films. In addition, we have shown that the weak nonradiative coupling between S_1 and S_0 appears to be associated with a substantial lattice distortion in the final compared to the initial state. This quinoid-like distortion is a result of exciton localization on only one chain at a time, but the short contact distance allows the exciton to hop between chains.

Acknowledgment. This work was supported by the NSF under Grant CHE-0615173; P.J.R. also acknowledges support from the R. A. Welch Foundation (F-0019).

References and Notes

(1) Schwartz, B. J. *Annu. Rev. Phys. Chem.* **2003**, *54*, 141.
(2) Brédas, J.-L.; Beljonne, D.; Coropceanu, V.; Cornil, J. *Chem. Rev.* **2004**, *104*, 4971.
(3) Cornil, J.; Heeger, A. J.; Brédas, J.-L. *Chem. Phys. Lett.* **1997**, *272*, 463–470.
(4) Cornil, J.; dos Santos, D. A.; Crispin, X.; Silbey, R.; Brédas, J.-L. *J. Am. Chem. Soc.* **1998**, *120*, 1289.
(5) Tretiak, S.; Saxena, A.; Martin, R. L.; Bishop, A. R. *J. Phys. Chem. B* **2000**, *104*, 7029.
(6) Hutchison, G. R.; Ratner, M. A.; Marks, T. J. *J. Am. Chem. Soc.* **2005**, *127*, 16866–16881.
(7) Brédas, J.-L.; Cornil, J.; Beljonne, D.; dos Santos, D. A.; Shuai, Z. *Acc. Chem. Res.* **1999**, *32*, 267.
(8) Lobaugh, J.; Rossky, P. J. *J. Phys. Chem. A* **1999**, *103*, 9432–9447.
(9) Lobaugh, J.; Rossky, P. J. *J. Phys. Chem. A* **2000**, *104*, 899–907.
(10) Sterpone, F.; Rossky, P. *J. Phys. Chem. B* **2008**, *112* (16), 4983.
(11) Oelkrug, D.; Tompert, A.; Gierschner, J.; Egelhaaf, H.-J.; Hanack, M.; Hohloch, M.; Steinhuber, E. *J. Phys. Chem. B* **1998**, *102*, 1902–1907.
(12) Bjorklund, T. G.; Lim, S.-H.; Bardeen, C. J. *Synth. Met.* **2004**, *142*, 195–200.
(13) Pariser, R.; Parr, R. G. *J. Chem. Phys.* **1953**, *21*, 466.
(14) Pariser, R.; Parr, R. G. *J. Chem. Phys.* **1953**, *21*, 767.
(15) Pople, J. A. *Trans. Faraday Soc.* **1953**, *49*, 1375.
(16) Warshel, A.; Karplus, M. *J. Am. Chem. Soc.* **1972**, *94*, 5612.
(17) Hurley, A. C. *Electronic Correlation in Small Molecules*; Academic Press: New York, 1976.
(18) By increasing the number of SCI states from 50 to 200, the energy gaps changed by only 2−3%. The electronic density of states computed *a posteriori* using a previously generated trajectory was demostrated to be visibly unchanged.
(19) Drukker, K. *J. Comput. Phys.* **1999**, *153*, 225.
(20) Allen, M. P.; Tildesely, D. J. *Computer Simulation of Liquids*; Oxford University Press: New York, 1987.
(21) Tully, J. C. *J. Chem. Phys.* **1990**, *93*, 1061.
(22) We use a fourth-order Runge−Kutta algorithm to integrate the time-dependent Schrödinger equation with 1000 intermediate time steps.
(23) Only transitions to the first three states are included since the description of higher-lying excited states within the SCI space is likely incomplete.
(24) Ruini, A.; Caldas, M. J.; Bussi, G.; Molinari, E. *Phys. Rev. Lett.* **2002**, *88*, 2064031.
(25) Bussi, G.; Ferretti, A.; Ruini, A.; Caldas, M. J.; Molinari, E. *Adv. Solid State Phys.* **2003**, *43*, 313–326.
(26) The fourth excited state, S_4, shows some charge-transfer character, as indicated by a substantial interchain transition dipole moment, but as it has no intensity in the GS absorption spectrum, we do not discuss it here.
(27) We decompose the vector between the centers of mass into parallel and orthogonal components to describe the sliding dynamics and contact distance, respectively. The parallel direction is chosen to be a unit vector pointing between the first and last carbon atoms on one chain, and the remainder of the joint center-of-mass vector is in the orthogonal direction; other reasonable definitions of these unit vectors yielded similar results.
(28) V_{ij} can spike one or more times prior to making the NA transition since the surface-hopping algorithm used is stochastic (see ref 21).
(29) Bjorklund, T.; Lim, S.-H.; Bardeen, C. *J. Phys. Chem. B* **2001**, *105*, 11970.
(30) Kersting, R.; Lemmer, U.; Mahrt, R. F.; Leo, K.; Kurz, H.; Bässler, H.; Göbel, E. O. *Phys. Rev. Lett.* **1993**, *70*, 3820.
(31) System renderings made with PyMOL, DeLano, W. L. http://www.pymol.org.

JP901229Z